ECOHYDROLOGY
Ecohydrol. **8**, 610–625 (2015)
Published online 1 August 2014 in Wiley Online Library
(wileyonlinelibrary.com) DOI: 10.1002/eco.1529

Long-term decrease in satellite vegetation indices in response to environmental variables in an iconic desert riparian ecosystem: the Upper San Pedro, Arizona, United States

Uyen Nguyen,[1] Edward P. Glenn,[1]* Pamela L. Nagler[2] and Russell L. Scott[3]

[1] *Department of Soil, Water and Environmental Science, The University of Arizona, Tucson, AZ, USA*
[2] *US Geological Survey, Southwest Biological Science Center, Sonoran Desert Research Station, Tucson, AZ, USA*
[3] *Southwest Watershed Research Center, USDA-Agricultural Research Service, Tucson, AZ, USA*

ABSTRACT

The Upper San Pedro River is one of the few remaining undammed rivers that maintain a vibrant riparian ecosystem in the southwest United States. However, its riparian forest is threatened by diminishing groundwater and surface water inputs, due to either changes in watershed characteristics such as changes in riparian and upland vegetation, or human activities such as regional groundwater pumping. We used satellite vegetation indices to quantify the green leaf density of the groundwater-dependent riparian forest from 1984 to 2012. The river was divided into a southern, upstream (mainly perennial flow) reach and a northern, downstream (mainly intermittent and ephemeral flow) reach. Pre-monsoon (June) Landsat normalized difference vegetation index (NDVI) values showed a 20% drop for the northern reach ($P < 0{\cdot}001$) and no net change for the southern reach ($P > 0{\cdot}05$). NDVI and enhanced vegetation index values were positively correlated ($P < 0{\cdot}05$) with river flows, which decreased over the study period in the northern reach, and negatively correlated ($P < 0{\cdot}05$) with air temperatures in both reaches, which have increased by 1·4 °C from 1932 to 2012. NDVI in the uplands around the river did not increase from 1984 to 2012, suggesting that increased evapotranspiration in the uplands was not a factor in reducing river flows. Climate change, regional groundwater pumping, changes in the intensity of monsoon rain events and lack of overbank flooding are feasible explanations for deterioration of the riparian forest in the northern reach. Copyright © 2014 John Wiley & Sons, Ltd.

KEY WORDS San Pedro River; Walnut Gulch Experimental Watershed; climate change; evapotranspiration; woody shrub encroachment; NDVI; enhanced vegetation index

Received 18 December 2013; Revised 19 June 2014; Accepted 21 June 2014

INTRODUCTION

Human activities and climate change have negatively impacted riparian forests throughout the world's arid and semiarid zones (Poff *et al*., 1997; Kingsford *et al*., 2006; Orellana *et al*., 2012; Perry *et al*., 2012). However, it is difficult to document long-term consequences of land use and climate change and to pinpoint environmental drivers of deterioration (Webb *et al*., 2007). Many cases of deterioration are due to direct impacts on river systems such as diversion of water for human use, flow regulation and introduction of invasive species (Poff *et al*., 1997). However, even unregulated and protected rivers can be impacted by regional and global changes in hydrology and climate (Perry *et al*., 2012).

A case in point is the Upper San Pedro River in northwestern Mexico and southeastern Arizona, United States. This river originates in Mexico and flows north into the United States, ultimately discharging into the Gila River in the Lower Colorado River Basin (Figure 1). Much of the riparian zone is protected within the San Pedro Riparian National Conservation Area (SPRNCA), a 55 km long portion of the river. Created in 1988, the SPRNCA is the United States' only designated Riparian National Conservation Area (Stromberg *et al*., 1996; Stromberg and Tellman, 2009). Agriculture, groundwater extraction and livestock grazing have been eliminated within the SPRNCA. However, regional groundwater pumping to support population growth and possible changes in climate in the area have raised concerns about the health of the riparian forest along the river (Stromberg *et al*., 2009a).

Numerous organized research efforts have been undertaken over the last couple of decades (e.g. Goodrich *et al*., 2000; Sorooshian *et al*., 2002) with the goal of determining the trajectory of ecological changes in the SPRNCA in response

*Correspondence to: Edward P. Glenn, Department of Soil, Water and Environmental Science, The University of Arizona, 1177 E. 4th Street, P. O. Box 210038, Tucson, AZ 85721-0038, USA.
E-mail: eglenn@ag.arizona.edu

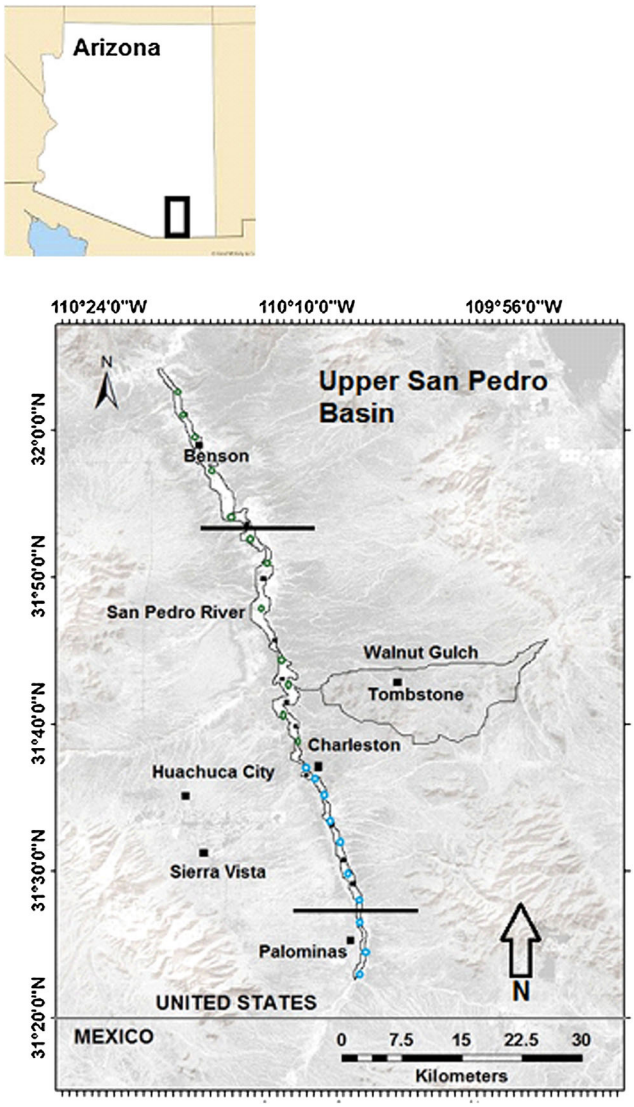

Figure 1. Locator map, showing shape file used to delineate riparian zone for Landsat and MODIS analyses. Closed black circles show location of MODIS pixels; open green circles show location of Landsat riparian sites in north reach; open blues circles show Landsat riparian sites in the south reach. Horizontal lines show north and south boundaries of the San Pedro Riparian National Conservation Area.

to land cover and land use changes (Kepner *et al*., 2000, 2002), hydrological factors (Hirschboeck, 2009; Mac Nish *et al*., 2009) and potential effects of climate change (Dixon *et al*., 2009). The scope of the studies encompassed the riparian zone itself as well as the tributary streams and the sparsely vegetated uplands (Leenhouts *et al*., 2006; Stromberg and Tellman, 2009; Serrat-Capdevil *et al*., 2011; see also special issues of *Agricultural and Forest Meteorology*, Goodrich *et al*., 2000, and *Water Resources Research*, Moran *et al*., 2008). The San Pedro is one of the best-studied rivers in the western United States. Nevertheless, most of the studies have been conducted over a relatively short period of time, and the longer-term trends in riparian vegetation cover and their relationship to meteorological and hydrological factors in the Upper San Pedro Basin are still in dispute (Thomas and Pool, 2006; Goodrich *et al*., 2008).

Concerns about the health of the riparian forest are partly due to an observed decrease in flows in the river over the past century (Thomas and Pool, 2006). Groundwater contributions to the river base flow (estimated as the lowest 7-day flow period of the year) decreased by 66% from 1942 to 2000 (Miller *et al*., 2002; Thomas and Pool, 2006), and in 2005, the US Geological Survey stream gauge (09471000) at Charleston in the SPRNCA recorded zero flow over a 7-day period for the first time since it was installed in 1904 (Mac Nish *et al*., 2009). Similar flow reductions did not occur in other southeastern Arizona and southwestern New Mexico rivers over the same period (Thomas and Pool, 2006). The long-term decrease includes decreases in total annual flows as well as base flows, but is due mainly to reductions in summer flows, while winter flows are so far unaffected (Thomas and Pool, 2006; Hirschboeck, 2009).

Rainfall has fluctuated over short and longer time scales over this period but has not shown an obvious trend in direction (Miller *et al*., 2002; Thomas and Pool, 2006; Goodrich *et al*., 2008). One hypothesis for the decrease in river flows is that velvet mesquite tree (*Prosopis velutina*) encroachment into the grasslands surrounding the river over the 20th Century has led to increased evapotranspiration (ET), reducing recharge to the river (Kepner *et al*., 2002; Thomas and Pool, 2006; Nie *et al*., 2012). Other possible causes for flow reductions are diminished intensity of individual monsoon rain events, reducing surface storm-water recharge even though total precipitation (PPT) has not changed (Goodrich *et al*., 2011) or lowering of groundwater levels near the river through regional pumping to support population growth in the watershed (Serrat-Capdevila *et al*., 2007; Mac Nish *et al*., 2009).

So far, a long-term trend towards deterioration of the riparian forest in response to reduced flows has not been detected. Jones *et al*. (2008) analysed changes in 'greenness' in the riparian corridor using normalized difference vegetation index (NDVI) values on Multi-Spectral Scanner Landsat images obtained for the 1973, 1986 and 1992 growing seasons. They compared the SPRNCA riparian zone with a portion of the riparian zone north of the SPRNCA, which is unprotected. They found little overall change in NDVI among years in combined areas, but noted a small but statistically significant ($P < 0{\cdot}05$) positive trend in the SPRNCA and a slightly negative trend in the unprotected control area. Kepner *et al*. (2002) reported a 2·6% increase in riparian plant cover in the whole basin between 1973 and 1992 based on classified Landsat images, and Stromberg *et al*. (2010) noted a historic trend towards expansion of the riparian forest in the San Pedro River. Hence, no clear downward trend in the

condition of the riparian vegetation has been detected despite the reduction in summer flows. In fact, reduced surface flows could conceivably be due to an increase in vegetation and ET in and along the riparian corridor (Thomas and Pool, 2006).

The goal of this study was to document long-term changes in green vegetation density in both the riparian corridor and in the surrounding uplands through satellite imagery, to shed light on the status of the riparian ecosystem and upland vegetation density that might be related to diminished flows. The specific objectives were as follows: (1) determine the multi-decadal trajectory of riparian and upland vegetation along the Upper San Pedro River based on satellite vegetation index values and (2) correlate vegetation index changes with concurrent hydrological and meteorological changes in the watershed.

MATERIALS AND METHODS

Overview of experimental design

The study employed data from the Landsat Thematic Mapper (TM) satellites and from the Moderate Resolution Imaging Spectrometer (MODIS) sensors on the Terra satellite. Landsat 5, the primary TM satellite used in this study, has provided coverage since 1984 at 30 m resolution, sufficient for mapping individual vegetation units. MODIS has provided coverage since 2000 at 250 m resolution but has near-daily coverage, so temporal coverage is much better than Landsat with a 16-day return time. Annual changes in NDVI and enhanced vegetation index (EVI) values in the riparian corridor were compared with changes in depth to water table (DTW), river flows (Flows), air temperature (T_{air}) and PPT to develop predictive models of the vegetation response to long-term trends in environmental variables. We divided the river into two reaches, one downstream (north) and one upstream (south) of the USGS streamflow-gaging station near Charleston, AZ, where a decrease in flows has been detected (Thomas and Pool, 2006). We also determined NDVI and EVI values for the upland areas in the watershed to see if decreased river flows are correlated with increased green vegetation density and therefore ET in the uplands (Nie *et al*., 2012).

Description of study area

The San Pedro River flows from south to north and extends for about 225 km, with a perennial flow over about 40% of its length (Stromberg and Tellman, 2009). The portion of the Upper San Pedro River considered in this study extends from Hereford, AZ, north of the United States/Mexico border, to just north of the city of Benson, AZ, a length of about 70 km (Figure 1). The watershed in this reach is divided into two sub-watersheds, the Sierra Vista Subwatershed to the south and upstream of the USGS Tombstone gauge (09471550) and the Benson Subwatershed to the north. River flows are due to surface runoff from the surrounding uplands and groundwater input from the regional aquifer, which is recharged primarily along the mountain fronts running parallel to the river delineating the watershed's east and west boundaries (Mac Nish *et al*., 2009). The climate is hot and dry. Annual PPT is about 300–400 mm year^{-1}, with about 60% arriving in summer monsoons, July–September, and 25% arriving in winter frontal storms (Scott *et al*., 2008).

The river consists of a main channel, which underwent entrenchment around the beginning of the 20th century, and surrounding terraces, corresponding to the width of the floodplain in the pre-entrenchment period. The channel is now 2–8 m below the upper terraces (Huckleberry *et al*., 2009). Vegetation consists of cottonwood (*Populus fremontii*) and willow (*Salix gooddingii*) trees plus understory shrubs and grasses near the active channel, and sacaton (*Sporobolus wrightii*) grasslands and velvet mesquite shrublands and woodlands growing further away from the channel on the pre-entrenchment terraces (Stromberg *et al*., 2006).

River flow varies from $<0{\cdot}5$ m^3 s^{-1} in May and June to >5 m^3 s^{-1} in August, with very high month to seasonal and inter-annual variability (Hirschboeck, 2009). The river is perennial in the reach south of Charleston, AZ, to Palominas near the United States - Mexico border, but is a mix of ephemeral, intermittent and perennial sections in the reach north of Charleston to Benson, Arizona (Figure 1). The northern reach was historically perennial but has been impacted by reduced flows since 1955 (Hirschboeck, 2009). The riparian vegetation is described in Stromberg *et al*. (2009b), groundwater hydrology is reviewed in Mac Nish *et al*. (2009) and flood flows are discussed in Hirschboeck (2009).

To represent the upland areas, we selected the region encompassed by the USDA-ARS Walnut Gulch Experimental Watershed, which is a major ephemeral tributary into the Upper San Pedro River. It is a 15·000 ha mosaic of mainly grasslands and shrublands, receiving about 350 mm year^{-1} of PPT (King *et al*., 2008). The main population centres are Sierra Vista and Fort Huachuca and their surrounding suburban areas. The population of Sierra Vista increased from about 3·100 in 1960 to nearly 50·000 in 2010 (US Census Bureau data), and nearby communities have expanded as well, for a total population of about 72·000 in the Sierra Vista sub-basin (Leenhouts *et al*., 2006).

Acquisition and processing of Landsat imagery

Landsat Thematic Mapper images (Path 35, Row 38) were obtained from the USGS Earth Explorer website (http://earthexplorer.usgs.gov/) (Table S1; supplemental tables and figures for the Materials and Methods section are labelled with S before the table or figure number). Images were supplied as Level 1T products. To assess

foliage density in the riparian corridor, one pre-monsoon image per year was obtained from 1984 to 2012. All images were from Landsat 5 except that the 2012 image was from ETM+ due to decommissioning of Landsat 5 in 2012. Except for 1985, images were all from June, corresponding to the usually cloudless period when phreatophytic trees (mesquite, cottonwoods and willows) are leafed out, but before the arrival of summer rains in July, which produce subsidiary greening from summer grasses and annuals (Scott *et al*., 2003; Gazal *et al*., 2006). In 1985, the June 7, 23 and July 9 images showed distorted colour values in the preview images, so the July 25 image was selected instead. Still, this image was near the beginning of the monsoon period.

Red, Blue and near infrared (NIR) bands on TM images were converted to calibrated radiance values using header information and algorithms in Chander and Markham (2003). TM bands were transformed using the cosine of the zenith sun angle combined with dark object subtraction model of Chavez (1996), for conversion of radiances to at-surface reflectance values. Two vegetation indices were used in this study: NDVI and EVI. NDVI is calculated as follows:

$$\mathrm{NDVI} = (\rho\mathrm{NIR} - \rho\mathrm{Red})/(\rho\mathrm{NIR} + \rho\mathrm{Red}) \quad (1)$$

where band values are expressed as reflectance values (ρ).

EVI was calculated from Red, Blue and NIR bands (Huete *et al*., 2011):

$$\mathrm{EVI} = G(\rho\mathrm{NIR} - \rho\mathrm{Red})/(\rho\ \mathrm{NIR} + C_1 \times \rho\mathrm{Red} + C_2 \times \rho\mathrm{Blue} + L) \quad (2)$$

where C_1 and C_2 are coefficients designed to correct for aerosol resistance, which uses the blue band to correct for aerosol influences in the red band. C_1 and C_2 have been set at -6 and 7·5, while G is a gain factor (set at 2·0 for Landsat and 2·5 for MODIS) and L is a canopy background adjustment set at (Huete *et al*., 2011).

An initial shape file of the riparian corridor (Figure 1) was prepared on the 1984 TM image by visually drawing the perimeter based on the contrast between the mesquite on the older, pre-entrenchment, alluvial terraces at the outer edge of the riparian corridor and the sparse shrubland in the adjacent uplands. Individual shape files of all the agricultural fields within the riparian corridor were prepared, and the area of riparian habitat was estimated as the difference between the total riparian zone area and the area of agricultural fields within the riparian zone. The riparian habitat consisted of vegetation as well as open water in the river channel and areas of bare soil within the incised channel. In order to sample just riparian vegetation, we created 22 additional shape files (Tables S2 and S3) that encompassed vegetation stands that were stable over the 1984–2012 study period. This was accomplished by delineating stands of plants on the 1984 image and then confirming that they still represented riparian vegetation on all images up to 2012 (i.e. had not been converted to agriculture or other land cover classes). In fact, all of the plant stands initially selected on the 1984 image were still present in 2012. Twelve of the sampled areas (Figure S1) were north of the Charleston gauge in the river reach containing mainly ephemeral and intermittent stretches, and 10 (Figure S2) were south of the gauge with mostly perennial flow reaches (Figure 1). These are named north (downstream) and south (upstream) reaches, respectively. The sampled areas extended across the terraces, incorporating both near-channel vegetation like cottonwood and willow, and vegetation on older alluvial terraces, like mesquite and sacaton grass areas above the incised channel.

An NDVI difference map of the whole riparian corridor was prepared by subtracting 1984 NDVI values from 2010 values on a pixel-by-pixel basis using ERDAS Imagine (Intergraph, Inc., Atlanta, GA, USA) software. Pixels that showed a 10% or greater increase in NDVI were coloured green, and those with a 10% or greater decrease in NDVI were coloured red to visually display vegetation changes (data for each shape file are in Tables S2 and S3). A 10% change threshold was selected because it was approximately equal to the mean net change in NDVI for all pixels over the study period and exceeds two times the 95% confidence interval of the mean NDVI so should represent a significant difference ($P < 0{\cdot}05$). Similar threshold criteria have been applied in other change-detection studies with satellite-derived NDVIs (e.g. Lunetta *et al*., 2006).

An additional Landsat image for each year from 1984 to 2012 was obtained during the July to September monsoon period to assess maximum rainfall-dependent foliage density of upland vegetation in the Walnut Gulch Experimental Watershed (WGEW), with the selection dependent on the best low-cloud-cover (Table S1). A shape file was prepared that encompassed the upland areas in the WGEW as delineated in Moran *et al*. (2008) to test the hypothesis that increases in mesquites in the uplands have led to decreasing river flows (Miller *et al*., 2002; Nie *et al*., 2012). Since mesquites green up from April to May in the uplands even in the absence of concurrent rains (Potts *et al*., 2008), the contrast between June and July–September NDVI values was used as an indicator of relative abundance of mesquites in the uplands.

Acquisition of MODIS pixels in the riparian zone

Moderate Resolution Imaging Spectrometer, with near-daily coverage of most of the earth, provides better temporal coverage than Landsat, with a composite image of cloud-free daily imagery available every 16 days. MODIS NDVI and EVI pixels were acquired at 10 additional sites in the riparian zone (Table S4). They were approximately evenly spaced within the riparian zone (Figure 1). Data were obtained from the Oak Ridge National Laboratory site (ORNL DAAC, 2013) in the form of MOD13Q1 16-day composite images

from 2000 to 2010. Pixel resolution is approximately 250 m. The ORNL MODIS subset tool displays the approximate pixel footprint area on a high-resolution image. We obtained data for single pixels located in stands of riparian vegetation but excluding pixels containing bare soil, open water or adjacent upland vegetation.

Single pixels are subject to gridding errors, as the geolocation error can be as great as 50 m at different acquisition dates (Tan *et al.*, 2006). In heterogeneous environments such as riparian corridors, this can introduce substantial variance in vegetation indices for single pixels in a series (Nagler *et al.*, 2014). However, multiple pixel arrays can capture non-riparian habitat in narrow corridors such as the San Pedro. Hence, our approach was to use single pixels arrayed over the riparian corridor rather than multiple pixel arrays in fewer locations or a single shape file prepared for the whole riparian corridor. This single-pixel approach has worked well in modelling patch-scale evapotranspiration dynamics measured by flux towers along the San Pedro (Scott *et al.*, 2008).

Additional imagery

High-resolution aerial and satellite images were examined to determine the nature of vegetation changes corresponding to increases or decreases in NDVI over time. Images were available from the Google Earth archives for the following times: November, 1992; May, 1996; September, 2003; and December, 2005 (USGS aerial photographs); June, 2006 and April, 2010 (USDA Farm Service Agency aerial photographs); June, 2011 (Digital Globe Quickbird satellite images); and April, 2013 (Spot satellite images). Cottonwoods and willows were easily distinguished from mesquites by the texture of their canopies, the shadows they cast and the fact that they appeared skeletonized (without leaves) in the winter image of December, 2005. Furthermore, the cottonwoods and willows tended to grow in narrow strands near the river, while mesquites grew on higher terraces away from the river. However, cottonwoods and willows could not be distinguished from each other.

Environmental data sources

Meteorological and hydrological data were generally from the same sources used in Miller *et al.* (2002) and Thomas and Pool (2006). Mean annual river flows were calculated from monthly flow values measured at the Charleston gauge station (USGS Site Number 09471000, 31·626°N, 110·174°W) obtained from the USGS Water Data for the Nation website (http://waterdata.usgs.gov/nwis). Data from 1905 to 2012 were used. Additional flow data were for the Palominas (USGS 09470500, 31·380°N, 110·111°W) gauge from the same data source. T_{air} was calculated from monthly means from the Tombstone NOAA Cooperative Station 028619 with data from 1932 to 2012. Air temperatures recorded at this station are similar to data from the WGEW (Goodrich *et al.*, 2008, 2011) but with a longer period of record. Total annual PPT and November to May PPT ($PPT_{N–M}$), defined as total PPT from November to May, were also from the Tombstone cooperative station for the riparian zone. PPT for the uplands in WGEW was the mean of Gauges 1–10 from the WGEW data base (http://www.tucson.ars.ag.gov/dap/).

Depth to water table was estimated from static water levels in wells selected along the river from south of Benson to Palominas near the Mexican border (Table S5). Well data were obtained from the USGS Water Data for the Nation website. Data for individual wells tended to be discontinuous over time, and most of the wells were installed 2000 or 2001, and the record for years before 2000 was discontinuous and represented by fewer wells. We calculated mean annual DTW from monthly observations for all years represented in the record of each well. Wells were selected which were within 200 m of the river. Wells tended to be clustered together with gaps between clusters. We selected the well nearest the river in each cluster and sampled well clusters at least 5 km apart from each other. Our final data set (Table S5) included a discontinuous set of 18 of the approximately 40 wells along the river from Benson to Palominas, documenting mean annual well levels from 1987 to 2012.

Statistical analyses

Statistical analyses followed procedures in Montgomery *et al.* (2006) and were implemented with SigmaPlot and Systat software (Systat, Inc., San Jose, CA, USA). Temporal trends in vegetation indices and environmental variables were tested by regressing mean annual values against year of measurement using linear least-squares analyses, with $P < 0{\cdot}05$ selected as the threshold for statistical significance. Relationships between NDVI and EVI and individual environmental variables were tested with correlation coefficients (r) with $P < 0{\cdot}05$ considered a significant correlation. The best combinations of environmental variables as predictors of NDVI and EVI were tested by multiple linear regressions analyses. We used a best-subsets procedure, in which all possible combinations of environmental variables were tested as predictors of the dependent variables. The best model was judged to be the one that had the highest adjusted r^2 and the lowest Mallows C_p coefficient (Mallows, 1973). This procedure protects against 'over-determining' the number of independent variables to include in the final model by penalizing models that have more rather than fewer explanatory variables in achieving nearly the same unadjusted r^2 (Montgomery *et al.*, 2006). Multicollinearity among independent variables was tested by computing the variable inflation factor (VIF), which measures the extent to which a single independent variable can be determined by the remaining individual variables. A VIF close to 1·0 means

the variable is independent of the remaining explanatory variables, while values above 4 are generally taken to indicate that the variable is not truly independent and should be excluded from the model or combined with one of the other explanatory variables (Craney and Surles, 2002). Multiple regression analyses also report the coefficients for each independent variable in the equation of best fit, the standard error of the mean (SEM) of each independent variable, the t value and the β coefficient. β coefficients gave an approximate estimate of the amount of variability in the dependent variable that is explained by each independent variable (Lane, 2013). Non-linear regression equations were fit to data using curve-fitting programs in SigmaPlot.

RESULTS

Landsat NDVI and EVI in the riparian zone, 1984–2012

Shape files based on the 1984 TM image showed that the riparian corridor covered 3951 ha, of which 2791 ha was riparian habitat and 1160 ha were agricultural fields within the riparian corridor. Both NDVI and EVI decreased significantly ($P < 0{\cdot}001$) over time in the riparian areas in the north reach (Figure 2A). After subtracting out the approximate value of bare soil (NDVI = 0·17 based on sampling non-vegetated areas within the riparian corridor), the mean NDVI for riparian vegetation decreased by about 20% from 1984 to 2012 (0·7% per year) ($r^2 = 0{\cdot}37$). NDVI did not decrease significantly ($P > 0{\cdot}05$) in the south reach; EVI decreased significantly ($P = 0{\cdot}007$) but with lower slope than the decrease for EVI in the north reach (Figure 2B). Vegetation indices of agricultural fields decreased by about 50% over the same time period ($r^2 = 0{\cdot}70$; Figure 3C). Most of the fields were still visible in the images, but they had much lower NDVI values than in the 1984 image, presumably because they were no longer cultivated.

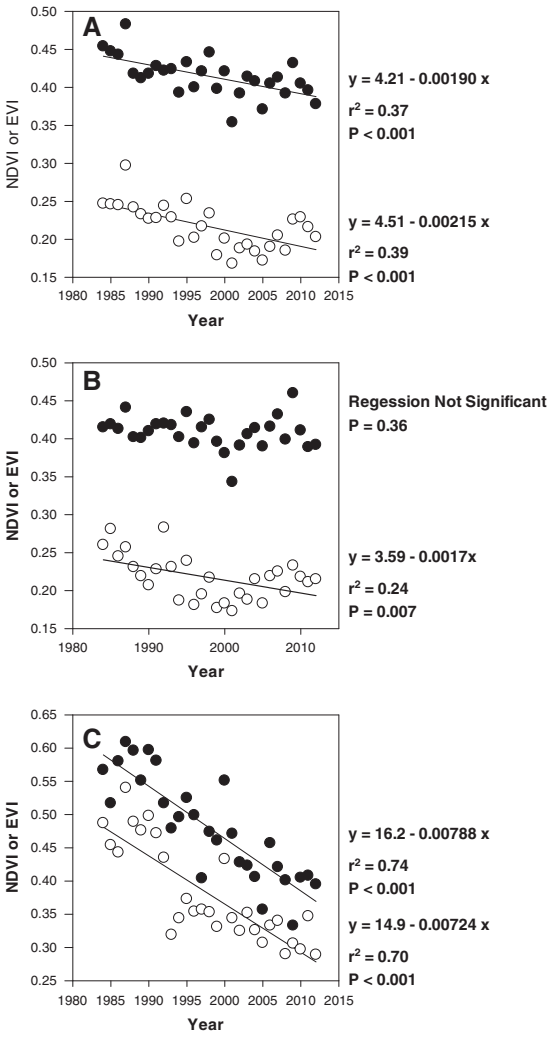

Figure 2. Trends in riparian normalized difference vegetation index (NDVI) (closed circles) and enhanced vegetation index (EVI) (open circles) in the north (A) and south (B) reaches of the riparian corridor of the San Pedro River, and trends in agricultural fields within the corridor (C) based on Landsat 5 Thematic Mapper images, 1984–2012.

NDVI differences maps

Normalized difference vegetation index difference maps comparing 1984 and 2010 are in Figure 3A (north reach) and B (south reach). For combined agriculture and non-agriculture classes in the riparian corridor, 926 ha were red (decreased NDVI) while 280 ha were green (increased NDVI). For the agriculture class, 737 ha were red and 181 ha were green, supporting the NDVI time-series showing retirement of fields. Most of the retired fields were in the south reach of the river, whereas some new fields (green pixels) appeared in the north reach. For the non-agriculture classes in the riparian zone, 189 ha were red and 99 ha were green. Thus, the pixel-by-pixel analysis qualitatively supports the NDVI trends in Figure 2, with both classes decreasing but with agriculture decreasing the most.

Red pixels accounted for 9·94% of total pixels in the north reach and 6·75% in the south reach, a difference that was not significant ($P = 0{\cdot}46$) (Table I; see Tables S2 and S3 for results for individual sites). However, green pixels accounted for only 0·726% of total pixels in the north reach and 2·71% in the south reach ($P = 0{\cdot}013$). The results reinforce the time-series data showing a long-term net decline in riparian NDVI, confined mainly to the north reach.

Examples of vegetation changes over time

Landsat imagery did not have sufficient resolution to determine which species increased or decreased. However, by comparing high-resolution archival imagery with Landsat NDVI difference maps, it was possible to

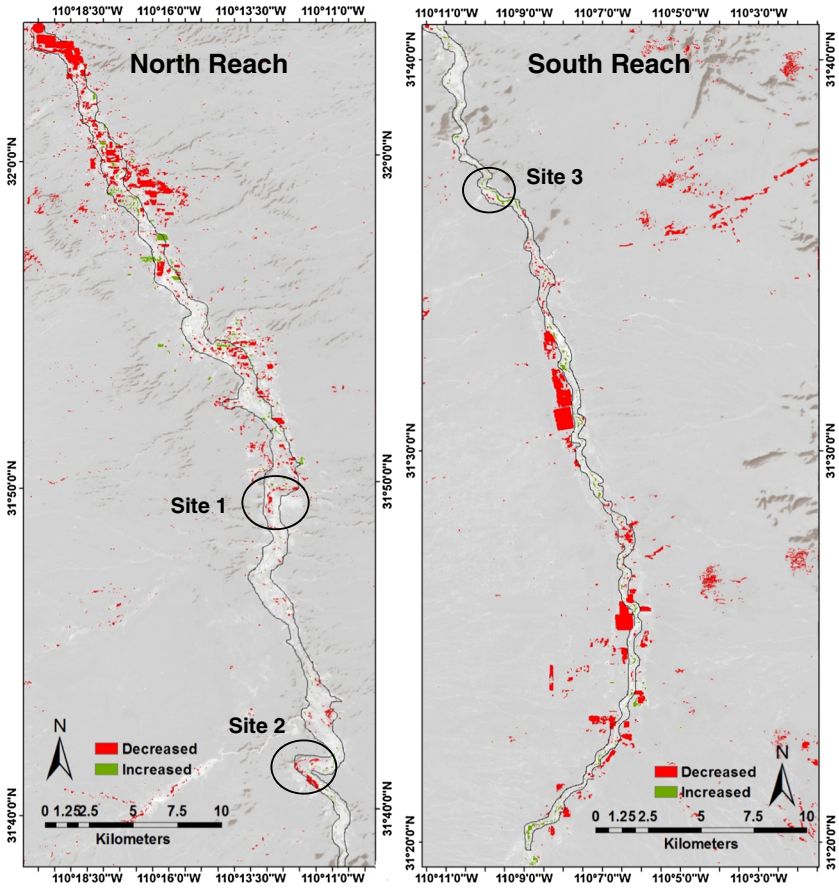

Figure 3. Enhanced vegetation index difference images of the San Pedro riparian corridor based on 1984 and 2012 Landsat 5 Thematic Mapper images. Green pixels had a 10% or greater increase in NDVI, while red pixels had a 10% or greater decrease in NDVI. Left and right panels show north and south reaches, respectively. Circles show areas selected for detailed comparison in Figures 4–6.

Table I. Percentage of pixels showing a 10% or greater decrease (red) or increase (green) in normalized difference vegetation index in the north and south reaches of the Upper San Pedro River in 2010 compared with 1984 Landsat images.

River reach	Red (%)	Green (%)
North	9·94 (3·24)	0·726 (0·206)a
South	6·75 (2·53)	2·71 (0·761)b
P	0·462	0·013

Values are means and standard errors of 12 (north) or 10 (south) individual sites; different letters after means denote significant differences at $P < 0{\cdot}05$.

qualitatively evaluate the nature of vegetation changes. Examination of archival high-resolution imagery showed that individual vegetation units were remarkably stable over time. Over the whole river, for example, most of the cottonwood trees visible on archival images dating from 1992 were still present in 2013. Examples of vegetation changes are in Figures 4–6, comparing archival imagery with NDVI difference images. At Site 1 in middle of the north reach (Figure 4A–C), cottonwoods fringing the river channel showed a net decrease in NDVI (Figure 4C), apparently because of the loss of individual trees over time, based on archival imagery (Figure 4A,B). At Site 2 further upstream (i.e. south) in the north reach, cottonwood trees showed an increase in NDVI, because of growth of tree canopies, whereas mesquite and grass stands away from the main channel decreased (Figure 5A–C). On the other hand, at Site 3 further upstream in the south reach, cottonwood trees along the main channel showed a clear increase in growth (Figure 6A,B) and NDVI (Figure 6C), while several trees away from the main channel apparently died by 2010.

Correlation of Landsat NDVI and EVI with environmental variables

Mean annual stream flow at the Charleston gauge has decreased by 62% since 1905 ($P < 0{\cdot}001$) (Figure 7A). Flows at the Charleston gauge decreased by 10·4% from 1984 to 2012 ($P = 0{\cdot}0037$), while flows at the Palominas gauge in the south reach did not decrease over their period of record (1951–1981, 1996–2012) ($P = 0{\cdot}437$). T_{air} at Tombstone increased over the whole period of record from 1932 to 2012

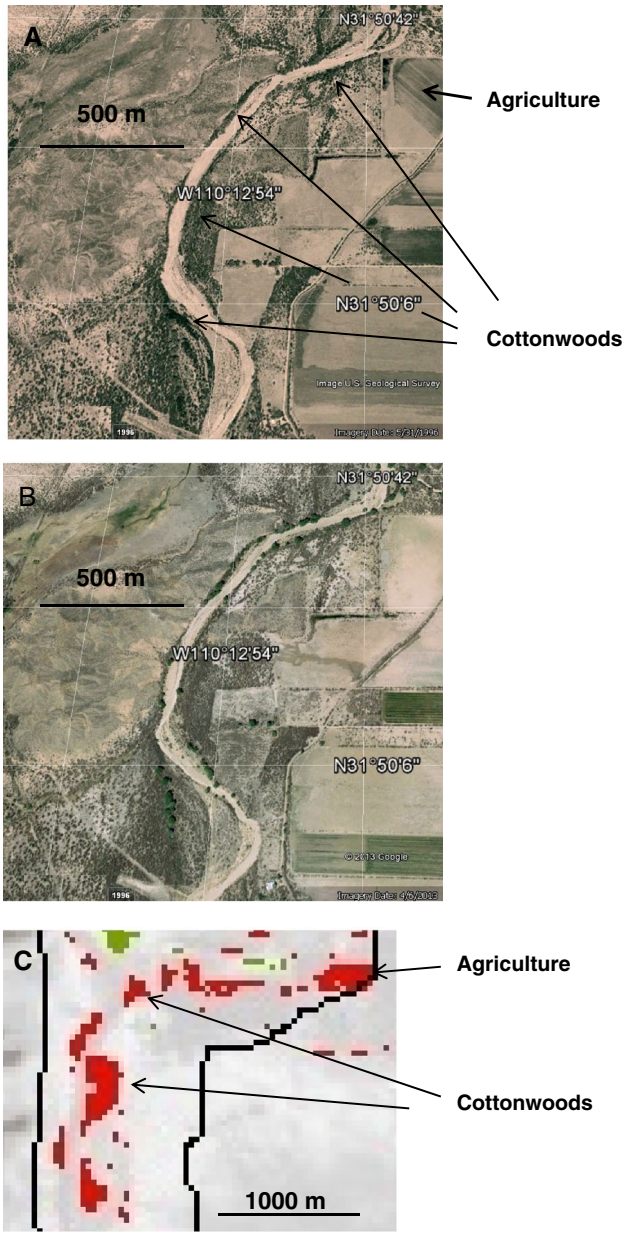

Figure 4. Example of decrease in normalized difference vegetation index (NDVI) due to the apparent loss of cottonwood or willow trees at Site 1 on the north reach of the San Pedro (upper circled area in Figure 3A). (A) is an aerial of the site in 1992; (B) is a Digital Globe image from 2013, showing apparent loss of trees (arrows); (C) shows a net decline in NDVI for the cottonwoods or willows along the river based on 1984 and 2010 Landsat images.

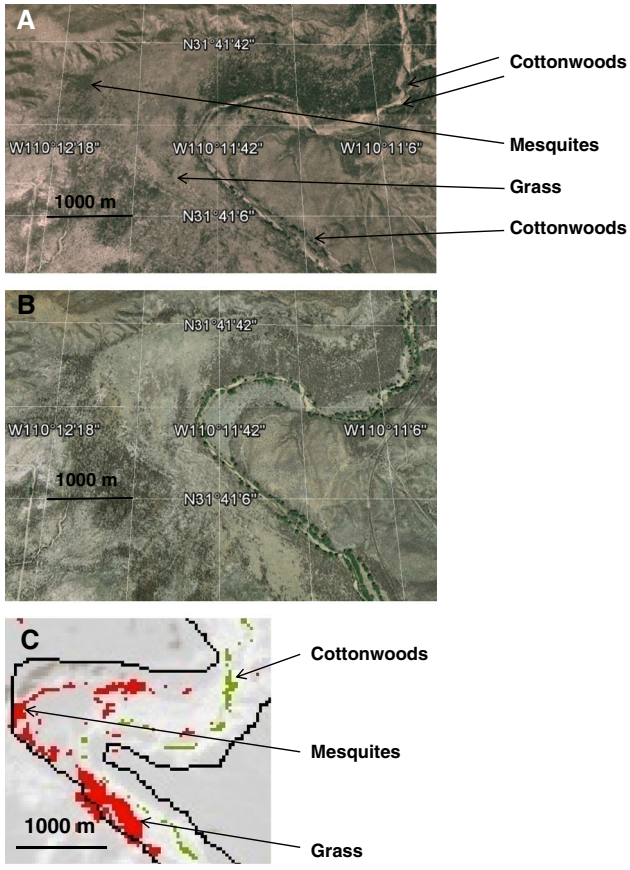

Figure 5. Example of increase in cottonwood normalized difference vegetation index (NDVI) and decreases in mesquite and grass NDVI at Site 2 in the north reach of the San Pedro River (lower circled area in Figure 3A). (A) is an aerial of the site in 1992; (B) is a Digital Globe image from 2013; (C) shows a net increase in NDVI for the cottonwoods or willows along the river and a decrease in mesquite and grass NDVI away from the river channel based on 1984 and 2010 Landsat images.

(Figure 7B), and from 1984 onward ($P < 0{\cdot}001$) at a mean rate of 0·00814 °C year^{-1}. On the other hand, PPT did not show a significant trend over either period ($P = 0{\cdot}88$ for 1931–2012; $P = 0{\cdot}097$ for 1984–2012) (Figure 7B). DTW for the wells surveyed in this study increased significantly from 1987 to 2012 ($P = 0{\cdot}046$) (Figure 7C). However, all of the increase occurred from 2005 to 2012 ($r^2 = 0{\cdot}96$, $P < 0{\cdot}001$) following a period of below-normal PPT. The well data were highly variable among locations, and it was not possible to resample the same wells over long time periods because of the short period of record of most of the wells.

Both NDVI and EVI decreased significantly by Year ($P < 0{\cdot}001$) (Table II). Annual variation in NDVI was significantly negatively correlated with T_{air} ($P < 0{\cdot}028$) and positively correlated with Flows at the Charleston gauge ($P = 0{\cdot}036$; Table II). A best-subsets multiple linear regression analysis with NDVI as the dependent variable showed that an equation containing T_{air} as a negative factor and Flows as a positive factor had the highest adjusted r^2 and the lowest C_p among all combinations of explanatory variables after excluding those with VIF > 4·0, but the explanatory power of the equation was low (adjusted $r^2 = 0{\cdot}18$; Table III). The only significant correlation between NDVI or EVI and environmental variables in the south reach was a negative correlation between EVI and T_{air} ($r = -0{\cdot}509$, $P = 0{\cdot}005$).

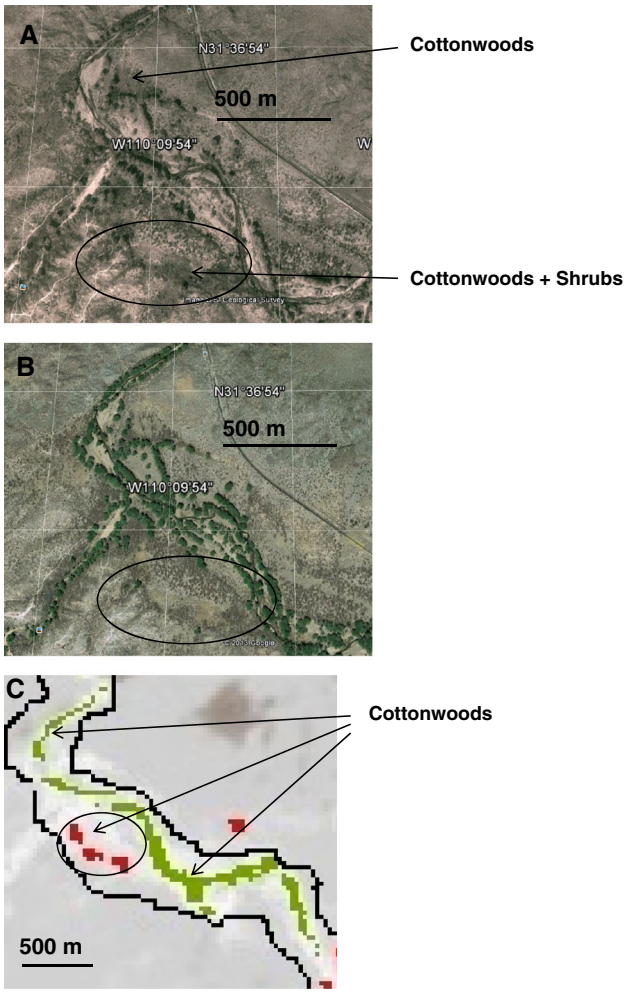

Figure 6. Example of increase in cottonwood normalized difference vegetation index (NDVI) at Site 3 in the south reach of the San Pedro River (circled area in Figure 3B). (A) is an aerial of the site in 1992; (B) is a Digital Globe image from 2013; (C) shows a net increase in NDVI for most of the cottonwoods or willows along the river but loss of trees and shrubs further away from the river (circled areas at bottom of A, B and C based on 1984 and 2010 Landsat images).

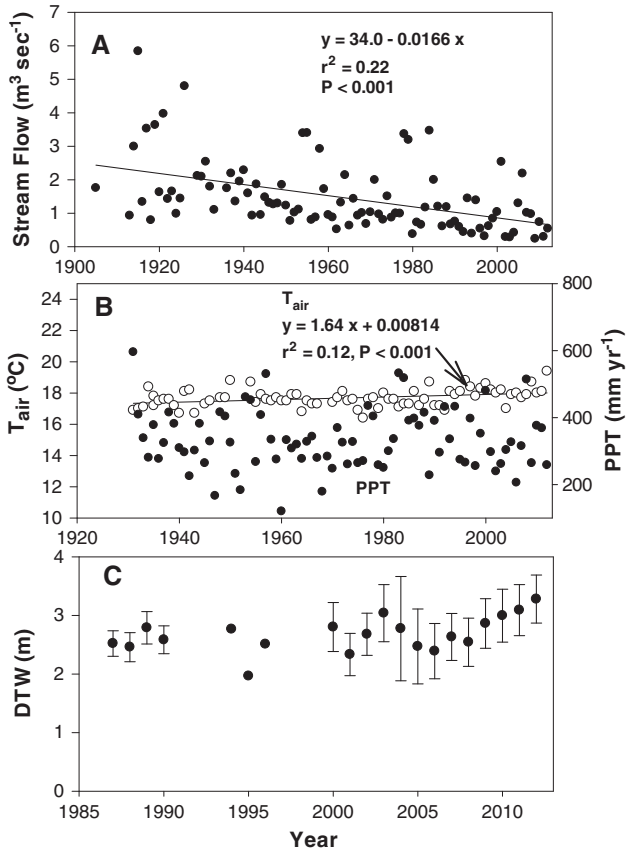

Figure 7. (A) Surface flows measured at the Charleston gauge on the San Pedro River; (B) mean annual air temperature (T_{air}) (open circles) and precipitation (PPT) (closed circles) at Tombstone, AZ; (C) depth to groundwater (DTW) in a sample of wells along the San Pedro River with standard errors (bars).

Correlation and regression of MODIS NDVI and EVI with environmental variables, 2000–2012

All variables showed year to year variations, but none showed a significant overall decrease or increase over the relatively short period of MODIS coverage (Figure 8). NDVI and EVI were closely correlated, as expected ($P < 0{\cdot}001$; Table IV). Correlations with environmental variables were slightly stronger for NDVI compared with EVI. NDVI was significantly negatively correlated with DTW ($P < 0{\cdot}048$) and positively correlated with mean annual flows (P 0·010). NDVI was marginally positively correlated with PPT ($P = 0{\cdot}064$).

The environmental variable that was most strongly correlated with NDVI was Flows, but the relationship was not linear; it was best predicted by an exponential rise to a maximum equation (Figure 9). NDVI reached a maximum at flows of about $1\,m^3\,s^{-1}$ The correlation coefficient between NDVI and the natural logarithm of Flows was 0·803 ($P < 0{\cdot}001$). A best-subsets multiple linear regression analysis showed that a combination of ln(Flows) and PPT as positive factors and DTW as a negative factor produced an equation with high predictive power (adjusted $r^2 = 0{\cdot}77$, $P < 0{\cdot}001$; Table V).

NDVI trends in Walnut Gulch uplands

June NDVI values, presumed to be primarily due to the green-up of any mesquite covered areas, decreased over this period, while July–September values did not show a significant trend (Figure 10A). Total annual PPT was variable over this period (Figure 10B), whereas $PPT_{N–M}$ decreased ($r = -0{\cdot}387$, $P = 0{\cdot}038$). June NDVI was significantly negatively correlated with T_{air} ($P < 0{\cdot}013$) and positively correlated with $PPT_{N–M}$ ($P < 0{\cdot}001$) but not with the current year's PPT ($P = 0{\cdot}46$) (Table VI). June NDVI was positively correlated with Flows, probably an indirect effect because Flows were positively correlated with PPT.

Table II. Correlation matrix of June Landsat riparian NDVI and EVI with meteorological and hydrological variables on the San Pedro River, 1984–2012.

	NDVI	EVI	Year	PPT	T_{air}	$T_{air(June)}$	Flows	DTW
NDVI	1·000	**0·861*****	**−0·611*****	0·218	**−0·378***	**−0·399***	**0·392***	−0·136
EVI		1·000	**−0·624*****	0·208	−0·335	−0·177	**0·385***	−0·128
Year			1·000	−0·314	**0·440***	0·0587	**−0·423***	**0·460***
PPT				1·000	−0·359	−0·210	**0·455***	−0·011
T_{air}					1·000	0·248	−0·344	0·421
$T_{air(June)}$						1·000	−0·364	0·207

PPT, precipitation; T_{air}, mean annual air temperature; $T_{air(June)}$, maximum June air temperature; Flows, river flows at the Charleston gauge; DTW, depth to groundwater of a sample of wells along the river; NDVI, normalized difference vegetation index; EVI, enhanced vegetation index. Asterisks denote significance at $P < 0·05$ (*), $P < 0·01$ (**) or $P < 0·001$ (***). Values with $P < 0.05$ are shown in bold.

Table III. Multiple linear regression analysis of June riparian Landsat NDVI, 1984–2012, with air temperature (T_{air}) and river flows (Flows) on the San Pedro River.

	Coefficient	Std. Error	β	t	P	VIF
Constant	0·659	0·149		4·419	< 0·001	-
T_{air}	−0·0140	0·00821	−0·31	−1·71	0·099	1·32
Flows	0·00755	0·00483	0·28	1·563	0·13	1·21

The equation of best fit was as follows: NDVI = 0·659–0·0140 T_{air} + 0·00755 Flows, adjusted $r^2 = 0·18$, SEM = 0·024, $P = 0·029$. $C_p = 2·02$.

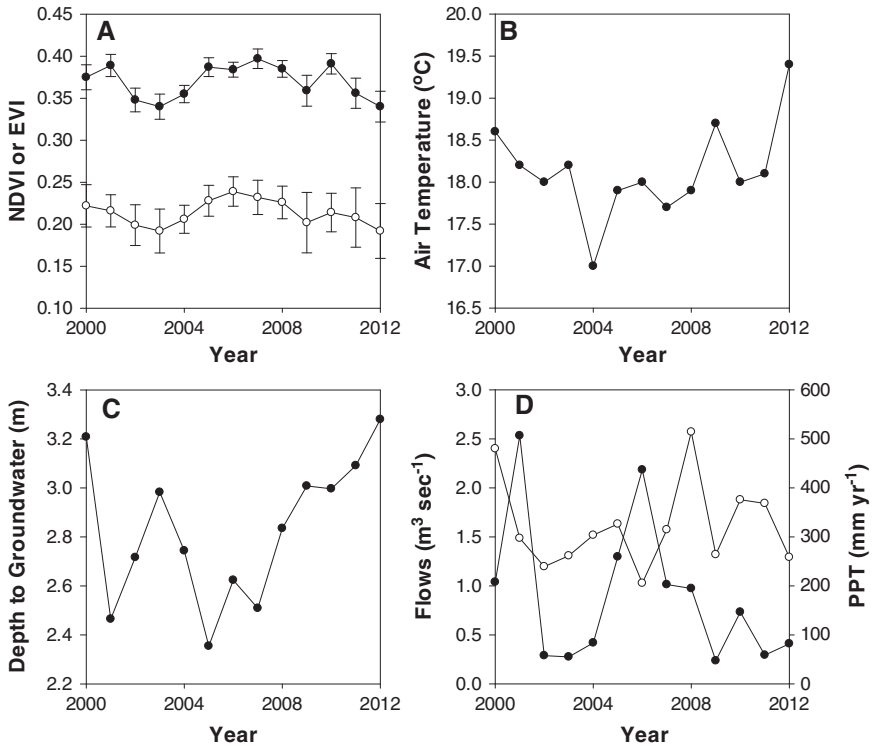

Figure 8. (A) Mean annual Moderate Resolution Imaging Spectrometer normalized difference vegetation index (NDVI) and enhanced vegetation index (EVI) with standard errors (bars) for 10 sites in the riparian corridor of the San Pedro River; (B) mean annual air temperature (T_{air}); (C) depth to groundwater (DTW); (D) river flows at the Charleston gauge (closed circles) and precipitation (PPT) at Tombstone (open circles).

Table IV. Correlation matrix of mean annual MODIS riparian NDVI and EVI with meteorological and hydrological variables on the San Pedro River, 2000–2012.

	NDVI	EVI	Year	PPT	T_{air}	Flows	DTW
NDVI	1·000	**0·885*****	−0·134 ns	0·528 ns	−0·304	**0·684****	−0·521
EVI		1·000	−0·121 ns	0·432 ns	−0·372	**0·679***	**−0·558***
Year			1·000	−0·225 ns	0·282	−0·341 ns	0·374
PPT				1·000	−0·053 ns	0·220 ns	0·244
T_{air}					1·000	−0·073 ns	**0·606***
Flows						1·000	**−0·595***

PPT, precipitation; T_{air}, mean annual air temperature; Flows, river flows at the Charleston gauge; DTW, depth to groundwater of a sample of wells along the river; NDVI, normalized difference vegetation index; EVI, enhanced vegetation index. Asterisks denote significance at $P < 0·05$ (*), $P < 0·01$ (**) or $P < 0·001$ (***). Values with $P < 0.05$ are shown in bold.

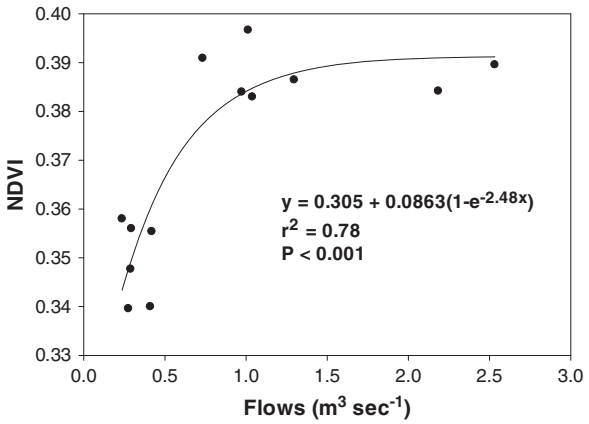

Figure 9. Exponential rise-to-a-max regression equation of Moderate Resolution Imaging Spectrometer riparian normalized difference vegetation index (NDVI) to mean annual river flows in the San Pedro River, 2000–2012.

However, Flows were included in the analysis to see if they were negatively correlated with June or July–September upland NDVI, which would be expected if increased upland ET (with NDVI as a surrogate) reduced river flows. The correlation coefficients between July and September NDVI and Flows was negative but non-significant ($P = 0·12$).

A best-subsets multiple linear regression analysis showed that an equation with T_{air} as a negative factor and $PPT_{N–M}$ as a positive factor was able to explain 43% June NDVI (Table VII). β coefficients showed that $PPT_{N–M}$ explained about three times as much of the annual variability in NDVI as T_{air}. On the other hand, July–September NDVI was not significantly correlated with any of the environmental variables used in this study, and no combination of variables produced significant regression equations in a best-subsets multiple linear regression analysis (not shown).

DISCUSSION

NDVI and EVI trends in the riparian corridor

Decreases in pre-monsoon NDVI and EVI of riparian vegetation proceeded steadily in the north reach from 1984 to 2012. The decrease occurred during the period of year when cottonwood (Gazal *et al.*, 2006) and mesquite trees (Scott *et al.*, 2004; Nagler *et al.*, 2005) have leafed out but before the arrival of monsoon PPT (Potts *et al.*, 2008), which augments groundwater supplies and provides a direct source of water in the vadose zone (Hirschboeck, 2009). Decreases in NDVI occurred in cottonwood as well as grass and mesquite stands.

Despite the decrease in NDVI in the north reach, individual plant stands in both north and south reaches showed remarkable stability over time, with most cottonwoods persisting for at least 20 years. The 22 plant stands outlined on the 1984 Landsat image were still present in

Table V. Multiple linear regression analysis of MODIS riparian NDVI, 2000–2012, with river flows (Flows) on the San Pedro River, depth to groundwater (DTW) and precipitation (PPT).

	Coefficient	Std. error	*β*	*t*	*P*	VIF
Constant	0·393	0·0199	–	19·7	< 0·001	–
ln(Flows)	0·0166	0·00397	0·632	4·17	0·002	1·18
DTW	−0·0137	0·00610	−0·335	−2·24	0·052	1·15
PPT	0·0000727	0·0000326	0·316	2·657	0·052	1·03

MODIS, Moderate Resolution Imaging Spectrometer; NDVI, normalized difference vegetation index. The equation of best fit was as follows: NDVI = 0·363 + 0·0166 ln(Flows) − 0·0137 DTW + 0·0000727 PPT, adjusted $r^2 = 0·77$, SEM = 0·010, $P < 0·001$, $C_p = 3·17$.

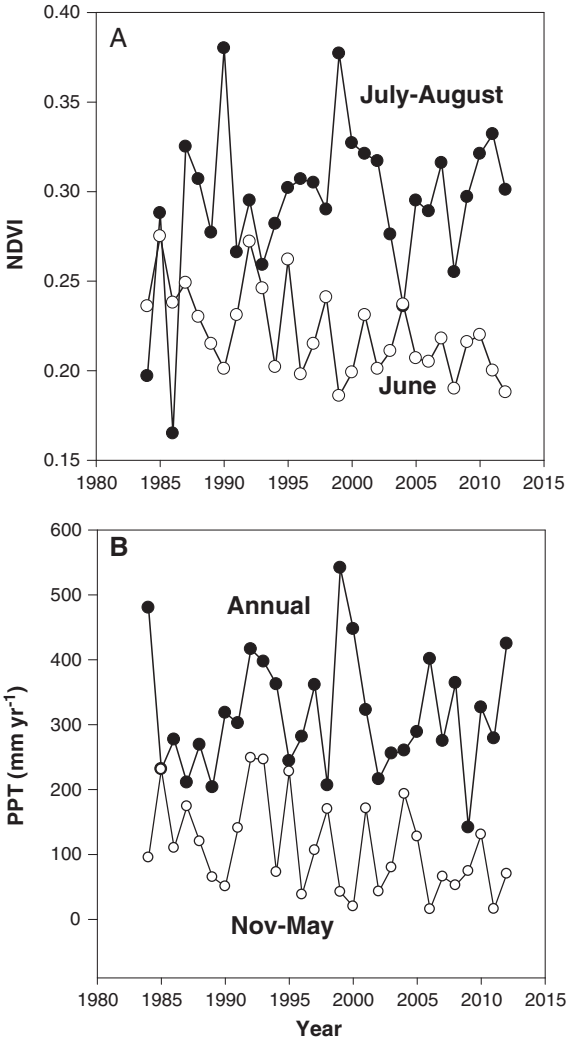

Figure 10. (A) June normalized difference vegetation index (NDVI) (open circles) and July–September NDVI (closed circles) over the Walnut Gulch Experimental Watershed by Landsat imagery, 1984–2012; (B) precipitation (PPT) at WGEW showing annual (closed circles) and fall–winter PPT (open circles).

2012, although with NDVI diminished by about 20% in the north reach. Flood flows have decreased in intensity since 1955 (Hereford and Betancourt, 2009), and the streambed is entrenched (Hereford and Betancourt, 2009), severely curtailing overbank flooding to rework alluvium and start new cohorts of trees on the terraces. This has resulted in a slow attrition of cottonwood trees at some sites and an ageing of tree cohorts that likely leads to decreased leaf area index (LAI) (Schaeffer *et al.*, 2000) and NDVI. At other sites where some recruitment has occurred, the tree canopies have increased in diameter, and NDVI has increased as well.

Stromberg *et al.* (2009a) predicted that successional changes will take place on the river, with the bands of cottonwoods and willows narrowing due to lack of overbank flooding. They also predicted that ageing stands of cottonwoods would be replaced by other patch types such as mesquites and grasslands. Our analysis supports these predictions and demonstrates that these processes are already underway. These results differ from Jones *et al.* (2008) who compared NDVI in the riparian corridor in 1973, 1986 and 1992, and did not detect large changes over time. However, our analyses would also fail to detect NDVI changes if based on only three images, because of the natural variability in NDVI among years (range over 28 images = 0·354–0·483). The results demonstrate the value of obtaining annual or more frequent imagery for vegetation change detection, because of the natural variability in seasonal and inter-annual NDVI.

The results also document a marked decline in agriculture along the San Pedro since 1984. Much of this decrease probably occurred after 1988 when the SPRNCA was created and agriculture fields within the conservation area were retired (Stromberg *et al.*, 1996; Stromberg and Tellman, 2009). So far, however, riparian vegetation does not seem to have reclaimed the cleared fields, which remain lightly vegetated.

Correlation and regression of riparian NDVI with environmental variables

Riparian NDVI and EVI were correlated with annual river flows in both the Landsat and MODIS series of images (Tables II and IV). Furthermore, flows at the Charleston gauge decreased from 1984 to 2012, as noted also in other

Table VI. Correlation matrix of pre-monsoon (June) and monsoon (July–September) Landsat upland NDVI with meteorological and hydrological variables at Walnut Gulch Experimental Watershed, 2000–2012.

	Pre-mon.	Mon.	Year	PPT	$PPT_{N–M}$	T_{air}	Flows
Pre-mon.	1·000	−0·333	**−0·649*****	0·082	**0·669*****	**−0·454***	**0·387***
Mon.		1·000	0·279	−0·157	−0·241	0·138	−0·293
Year			1·000	−0·314	−0·387*	**0·440***	**−0·423****
PPT				1·000	0·056	−0·359	**0·455***
$PPT_{N–M}$					1·000	0·040	−0·293

PPT, precipitation; $PPT_{N–M}$, November to May PPT; T_{air}, mean annual air temperature; NDVI, normalized difference vegetation index. Asterisks denote significance at $P < 0·05$ (*) or $P < 0·01$ (**).

Table VII. Multiple linear regression of June upland Landsat NDVI from 1984 to 2012 with T_{air} and November to May precipitation ($PPT_{N–M}$) at the Walnut Gulch Experimental Watershed.

	Coefficient	Std. error	β	*t*	*P*	VIF
Constant	0·610	0·122	–	6·27	< 0·001	–
T_{air}	−0·0243	0·00663	−0·177	−1·10	< 0·284	1·29
PPT_{FW}	0·000132	0·0000546	0·585	3·82	< 0·001	1·29

NDVI, normalized difference vegetation index. The equation of best fit was as follows: NDVI = 0·430 - 0·00726 T_{air} + 0·000197 PPT_{FW}, adjusted $r^2 = 0·43$, SEM = 0·018, $P < 0·001$. $C_p = 2·19$.

studies (Thomas and Pool, 2006; Goodrich *et al*., 2011). By contrast, flows at the Palominas gauge did not decrease over their period of record, and the south reach of the river as defined in this study is still mostly perennial (Stromberg *et al*., 2009b). The equation of best fit between NDVI and flows was an exponential rise-to-a-max equation, with an inflection point at about 1 $m^3 s^{-1}$. This threshold-like behaviour likely indicates that most of the time, the riparian vegetation has all the water it needs from the alluvial aquifer, but in drought/low-flow years, these phreatophytes are negatively impacted. Decreases in NDVI can be due to a lower LAI or to lower leaf water contents due to water stress. Hence, there appears to be a critical value for surface flows needed to recharge the alluvial aquifer to support riparian ET. Surface flood flows have been shown to be important for recharging the San Pedro alluvial aquifer (Baillie *et al*., 2007).

Depth to water table was also a significant negative factor in explaining the reduction in EVI in the MODIS series (Table IV). DTW was negatively correlated with river flows and increased between 2005 and 2012. However, the DTW record is discontinuous, and few wells have been monitored for long time periods, and no clear statistical trend was evident in the long-term well record. Mean DTW is currently between 2 and 3 m, sufficient to sustain cottonwoods and willows (Stromberg *et al*., 1996; Snyder and Williams, 2000; Williams and Scott, 2009), but if the recent trend of increasing DTW continues, those trees can be expected to eventually decrease in the riparian zone (Stromberg *et al*., 1996, 2006, 2009a,b). Mac Nish *et al*. (2009) showed that 50 years of groundwater pumping has created a basin-wide cone of depression of the regional aquifer that they suggested was a key cause of base flow decline in the river. PPT was also a positive predictor of MODIS NDVI. These riparian species plants depend primarily on groundwater, which is replenished by the regional aquifer as well as surface runoff, but they also respond to PPT that increases soil moisture in the vadose zone (Williams and Scott, 2009).

June riparian NDVI was negatively correlated with T_{air} in the Landsat series, although the correlation coefficient was low. The increases in T_{air} over the Landsat and MODIS periods of record were both low, under 0·5 °C. However, the positive trend noted for Tombstone data has been confirmed by long-term monitoring at temperature stations distributed throughout the WGEW (Goodrich *et al*., 2008, 2011). Even desert-adapted plants are subject to stress effects because of high summer temperature and low humidity, a condition referred to as 'atmospheric drought' (Naithani *et al*., 2012). In hot, dry air, the vapour pressure deficit in the atmosphere exceeds the capacity of even well-adapted plants to meet atmospheric water demand, and they respond through partial stomatal closure in the middle of the day, especially in plants already subject to moisture stress (Glenn *et al*., 2013). Barron-Gafford *et al*. (2012) showed that net assimilation of carbon was inhibited at leaf temperature over 30 °C for both mesquites and grasses along the San Pedro, especially in the dry pre-monsoon period, and these temperatures are frequently exceeded in summer. Eventually, this stress effect could be manifested as a reduction in LAI that could be detected as a reduction in NDVI or EVI. Determining if this is the case along the San Pedro is important given the likely further increases in T_{air} due to global warming (Barron-Gafford *et al*., 2012).

Correlation and regression of upland NDVI with environmental variables

June NDVI in WGEW decreased by about 20% over the period 1984–2012, correlated with increased T_{air} as a negative factor and November to May PPT as a positive factor. Green-up of upland mesquites occurs in April–June during the spring drought, but they usually do not show significant levels of transpiration or carbon exchange until the arrival of the monsoons (Potts *et al*., 2008). Their pre-monsoon green-up depends on soil moisture carried over from the previous fall and winter PPT, explaining the correlation between June NDVI and $PPT_{N–M}$. Grasses also have a partial green-up ahead of the monsoons (Hamerlynck *et al*., 2013), so the June NDVI response is not due to mesquites alone. As with riparian plants, T_{air} in WGEW exceeded the optimal value for photosynthesis in June (Barron-Gafford *et al*., 2012), explaining the negative correlation between June NDVI and T_{air}. On the other hand, July–September upland NDVI was not correlated with any of the environmental variables. A positive correlation is expected between NDVI and PPT (Peters

and Eve, 1995), but single Landsat scenes during the monsoon season would not necessarily capture the overall seasonal response to PPT.

Are reduced river flows a consequence of increased ET in the uplands or riparian zone?

The hypothesis that mesquite encroachment into the surrounding grasslands is responsible for reduced river flows (Nie *et al*., 2012) depends on two assumptions. The first is that mesquite cover has actually increased in the uplands over the time when flows were diminishing. Support comes from Kepner *et al*. (2000, 2002) who used a pixel-classification program to detect land cover changes based on Landsat images from 1973, 1986 and 1992. They reported that between 1973 and 1992, mesquite cover increased from 2·75% to 14% of total land cover in the Upper San Pedro Watershed, while grass cover decreased from 41% to 35%. However, King *et al*. (2008), relying primarily on archival photographs and ground transect data, concluded that any large-scale change in vegetation in WGEW (a subunit of the larger watershed) must have taken place before 1967 and that vegetation communities have been relatively stable since then. Contrary to Kepner *et al*. (2000, 2002; Nie *et al*., 2012), they concluded that widespread encroachment of mesquites has not occurred in the WGEW grasslands.

The second assumption is that mesquite-encroached grasslands have higher ET rates than non-encroached grasslands. Nie *et al*. (2012) used a soil–water–atmosphere transfer (SWAT) simulation model to show that as mesquite encroachment into grasslands was increased from 0% to 100% within their model watershed, simulated ET increased, while runoff and percolation (groundwater recharge) decreased. Their parameterization of the SWAT model assigned higher LAI and hence higher ET for mesquite compared with grasses, and they cited Scott *et al*. (2006) as support for the assumption that mesquites have higher ET than grasses. However, the Scott *et al*. (2006) study was conducted in the riparian corridor of the river where mesquites have access to groundwater and does not necessarily apply to the uplands where plants are rainfall-limited. A direct comparison of ET between a grassland, shrubland and mesquite-encroached grassland in the uplands of this region reveals that, within the uncertainty of the measurements, essentially all of the PPT minus the local storm runoff is returned back to the atmosphere via ET regardless of the vegetation type (Scott, 2010).

In the present study, June NDVI of upland vegetation, representing mesquites plus other plants with early green-up, decreased from 1984 to 2012 at the same time as river flows and riparian NDVI decreased. Plant transpiration accounts for 60% to 80% of ET in these uplands (Moran *et al*., 2009; Cavanaugh *et al*., 2011), and ET is strongly correlated with NDVI in the both the WGEW uplands (Nagler *et al*., 2007) and the riparian corridor (Nagler *et al*., 2005). To the extent that green plant cover determines ET, our study does not support the hypothesis that increased ET in either the riparian zone or due to mesquite encroachment in the uplands is responsible for reduced river flows. However, we did not directly measure ET or project NDVI over complete growing seasons. It is possible that other factors (e.g. increase in the length of the growing season) could lead to an increase in regional ET even if plant cover does not increase. Further research determining the actual extent of mesquite encroachment in the study area, and a more detailed upland mesquite and grass ET comparison, is needed to resolve this controversy.

Causes and consequences of future decreases in river flows

Relationships between river flows, groundwater and riparian NDVI and EVI suggest that decreasing surface flows and rates of alluvial aquifer recharge is already impacting the riparian forest, at least during the pre-monsoon period, especially in the northern reach. As noted by Thomas and Pool (2006), agricultural pumping is a relatively small term in the water budget, and agricultural NDVI decreased by 50% from 1984 to 2012, so it cannot explain the magnitude of the reduction in river flows or riparian NDVI, or the increase in DTW. Changes in vegetation do not seem to be sufficient to explain decreases in San Pedro River flows at least from 1984 to the present, and the trend towards less-intense rainfall events did not extend beyond 1998 (Goodrich *et al*., 2008), but decreases in river flows have continued. The cause or causes of the reduction in river flows remain uncertain (Thomas and Pool, 2006; Stromberg *et al*., 2009b; Goodrich *et al*., 2011), but future research should continue to focus on the relationship between regional pumping, flows in the river and the health of the riparian forest in SPRNCA. The present study shows that a slow decline in riparian vegetation, predicted by Stromberg *et al*. (2009a) based on flow reductions and lack of recruitment of new cohorts of phreatophytes, is already in progress.

ACKNOWLEDGEMENTS

Any use of trade, product or firm names is for descriptive purposes only and does not imply endorsement by the US Government. USDA is an equal opportunity employer.

REFERENCES

Baillie MN, Hogan JF, Ekwurzel B, Wahi AK, Eastoe CJ. 2007. Quantifying water sources to a semiarid riparian ecosystem, San Pedro River, Arizona. *Journal of Geophysical Research – Biogeosciences* **112**: G03S02. DOI: 10.1029/2006JG00026

Barron-Gafford GA, Scott RL, Jenerette GD, Huxman TE. 2012. Temperature and precipitation controls over leaf- and ecosystem-level

CO_2 flux along a woody plant encroachment gradient. *Global Change Biology* **18**: 1389–1400.
Cavanaugh ML, Kurc SA, Scott RL. 2011. Evapotranspiration partitioning in semiarid shrubland ecosystems: a two-site evaluation of soil moisture controls on transpiration. *Ecohydrology* **4**: 671–681.
Chander G, Markham B. 2003. Revised Landsat-5 radiometric calibration procedures and postcalibration dynamic ranges. *IEEE Transactions on Geoscience and Remote Sensing* **41**: 2674–2677.
Chavez Jr. PS. 1996. Image-based atmospheric corrections: revisited and improved. *Photogrammetric Engineering and Remote Sensing* **62**: 1025–1036.
Craney TA, Surles JG. 2002. Model-dependent variance inflation factor cutoff values. *Quality Engineering* **14**: 391–403.
Dixon MD, Stromberg JC, Price JT, Galbraith H, Fremier AK, Larsen EW. 2009. Potential effects of climate change on the Upper San Pedro Riparian ecosystem. In *Ecology and Conservation of the San Pedro River*, Stromberg JC, Tellman B (eds). University of Arizona Press: Tucson, AZ; 57–72.
Gazal RM, Scott RL, Goodrich DC, Williams DG. 2006. Controls on transpiration in a semiarid riparian forest. *Agricultural and Forest Meteorology* **137**: 56–67.
Glenn EP, Nagler PL, Morino K, Hultine KR. 2013. Phreatophytes under stress: transpiration and stomatal conductance of saltcedar (*Tamarix* spp.) in a high-salinity environment. *Plant and Soil* **371**: 658–672.
Goodrich DC, Chehbouni A, Goof B, Mac Nish D, Maddock T, Moran S. 2000. Preface to the Semi-Arid Land-Surface-Atmosphere (SALSA) program special issue. *Journal of Agricultural and Forest Meteorology* **105**: 3–20.
Goodrich DC, Unkrich CL, Keefer TO, Nichols MH, Stone JJ, Levick LR. 2008. Event to multidecadal persistence in rainfall and runoff in southeast Arizona. *Water Resources Research* **44**: W05514.
Goodrich DC, Marks D, Seyfried MS, Keefer TO, Unkrich CL, Clark PE. 2011. Utilizing long-term ARS data to compare and contrast hydroclimatic trends from snow and rainfall dominated watersheds. In *Proceedings of the 4th Interagency Conference of Research in the Watersheds*, Medley CN, Patterson G, Parker MJ (eds). U.S. Department of Interior Scientific Investigations Report 2011-5169: Reston, VA; 13–39.
Hamerlynck EP, Scott RL, Barron-Gafford GA. 2013. Consequences of cool-season drought-induced plant mortality to Chihuahuan Desert grassland ecosystem and soil respiration dynamics. *Ecosystems* **16**: 1178–1191.
Hereford R, Betancourt JL. 2009. Historic geomorphology of the San Pedro River. In *Ecology and Conservation of the San Pedro River*, Stromberg JC, Tellman B (eds). University of Arizona Press: Tucson, AZ; 232–250.
Hirschboeck KK. 2009. Flood flows of the San Pedro River. In *Ecology and Conservation of the San Pedro River*, Stromberg JC, Tellman B (eds). University of Arizona Press: Tucson, AZ; 300–312.
Huckleberry G, Lite SJ, Katz G, Pearthree P. 2009. Fluvial geomorphology. In *Ecology and Conservation of the San Pedro River*, Stromberg JC, Tellman B (eds). University of Arizona Press: Tucson, AZ; 251–267.
Huete AR, Didan K, van Leeuwem W, Miura T, Glenn EP. 2011. MODIS vegetation indices. *Land Remote Sensing and Environmental Change* **11**: 579–602.
Jones BK, Edmonds CE, Slonecker ET, Wickham JD, Neale AC, Wade TG, *et al*. 2008. Detecting changes in riparian habitat conditions based on patterns of greenness change: a case study from the Upper San Pedro River Basin, USA. *Ecological Indicators* **8**: 89–99.
Kepner WG, Watts CJ, Edmonds CM, Maingi JK, Marsh SE, Luna G. 2000. A landscape approach for detecting and evaluating change in a semi-arid environment. *Environmental Monitoring and Assessment* **64**: 179–195.
Kepner WG, Edmonds CM, Watts CJ. 2002. Remote sensing and geographic information systems for decision analysis in public resource administration: a case study of 25 years of landscape change in a southwestern watershed. EPA 600 R-12/039, U.S. Environmental Protection Agency, Office of Research and Development, Las Vegas, NV.
King DM, Skirvin SM, Collins CD, Moran MS, Biedenbender SH, Kidwell MR, *et al*. 2008. Assessing vegetation change temporally and spatially in southeastern Arizona. *Water Resources Research* **44**: W05S15.
Kingsford RT, Lemly AD, Thompson JR. 2006. Impacts of dams, river management and diversions on desert rivers. In *Ecology of Desert Rivers*, Kingsford RT (ed.). Cambridge University Press: Cambridge, UK; 203–247.
Lane DM. 2013. *Online Statistics Education: A Multimedia Course of Study*. Rice University: Houston, TX. (http://onlinestatbook.com/)
Leenhouts JM, Stromberg JC, Scott RL (eds). 2006. *Hydrologic Requirements of and Consumptive Ground Water Use by Riparian Vegetation along the San Pedro River, Arizona*. U.S. Geological Survey Scientific Investigations Report, 2005-5163: Reston, VI; 154.
Lunetta RS, Knight JF, Ediriwickrema J, Lyon JG, Worthy LD. 2006. Land-cover change detection using multi-temporal MODIS NDVI data. *Remote Sensing of Environment* **106**: 142–154.
Mac Nish R, Baird KJ, Maddock T. 2009. Groundwater hydrology of the San Pedro River Basin. In *Ecology and Conservation of the San Pedro River*, Stromberg JC, Tellman B (eds). University of Arizona Press: Tucson, AZ; 285–299.
Mallows CL. 1973. Some comments on C_p. *Technometrics* **15**: 661–675.
Miller SC, Kepner WG, Mehaffey MH, Hernandez M, Miller RC, Goodrich DC, *et al*. 2002. Integrating landscape assessment and hydrologic modeling for land cover change analysis. *Journal of the American Water Resources Association* **38**: 915–929.
Montgomery DC, Peck EA, Vining GG. 2006. *Introduction to Linear Regression Analysis*. John Wiley & Sons: New York.
Moran MS, Emmerich WE, Goodrich DC, Heilmman P, Colling CH, Keefer TO, *et al*. 2008. Preface to special issue on fifty years of research and data collection: U.S. Department of Agriculture Walnut Gulch Experimental Watershed. *Water Resources Research* **44**: W055S01.
Moran MS, Scott RL, Keefer TO, Emmerich WE, Hernandez M, Nearing GS, Paige G, Cosh MH, O'Neal PE. 2009. Partitioning evapotranspiration in semiarid grassland and shrubland ecosystems using time series of soil surface temperature. *Agricultural and Forest Meteorology* **149**: 59–72.
Nagler PL, Scott RL, Westenburg C, Cleverly JR, Glenn EP, Huete AR. 2005. Evapotranspiration on western US rivers estimated using the enhanced vegetation index from MODIS and data from eddy covariance and Bowen ratio flux towers. *Remote Sensing of Environment* **97**: 337–351.
Nagler PL, Glenn EP, Kim H, Emmerich W, Scott RL, Huxman TE, *et al*. 2007. Relationship between evapotranspiration and precipitation pulses in a semiarid rangeland estimated by moisture flux towers and MODIS vegetation indices. *Journal of Arid Environments* **70**: 443–462.
Nagler PL, Pearlstein S, Glenn EP, Brown TB, Bateman HL, Bean DW, Hultine KR. 2014. Rapid dispersal of saltcedar (*Tamarix* spp.) biocontrol beetles (*Diorhabda carinulata*) on a desert river detected by phenocam, MODIS imagery and ground observations. *Remote Sensing of Environment* **140**: 2006–219.
Naithani KJ, Ewers BE, Pendall E. 2012. Sap flux-scaled transpiration and stomatal conductance response to soil and atmospheric drought in a semi-arid sagebrush ecosystem. *Journal of Hydrology* **464**: 176–185.
Nie W, Yuan Y, Kepner W, Erickson C, Jackson M. 2012. Hydrological impacts of mesquite encroachment in the upper San Pedro watershed. *Journal of Arid Environments* **82**: 147–155.
Oak Ridge National Laboratory Distributed Active Archive Center (ORNL DAAC). 2013. MODIS subsetted land products, Collection 5. Available online http://daac.ornl.gov/MODIS/modis.html from ORNL DAAC, Oak Ridge, Tennessee, U.S.A. Accessed September 13, 2013.
Orellana F, Verma P, Loheide SP, Daly E. 2012. Monitoring and modeling water–vegetation interactions in groundwater-dependent ecosystems. *Reviews in Geophysics* **50**: RG3003.
Perry LG, Andersen DC, Reynolds LV, Nelson SM, Shafroth PB. 2012. Vulnerability of riparian ecosystems to elevated CO_2 and climate change in arid and semiarid western North America. *Global Change Biology* **18**: 821–842.
Peters AJ, Eve MD. 1995. Satellite monitoring of desert plant community response to moisture availability. *Environmental Monitoring and Assessment* **37**: 273–287.
Poff NL, Allen JD, Bain MB, Karr JR, Prestegaard KL, Richter BD, *et al*. 1997. The natural flow regime. *Bioscience* **47**: 769–784.
Potts DL, Scott RL, Cable JM, Huxman TE, Williams DG. 2008. Sensitivity of mesquite shrubland CO_2 exchange to precipitation in contrasting landscape settings. *Ecology* **89**: 2900–2910.
Schaeffer SM, Williams DG, Goodrich DC. 2000. Transpiration of cottonwood/willow forest estimated from sap flux. *Agricultural and Forest Meteorology* **105**: 257–270.

Scott RL. 2010. Using watershed water balance to evaluate the accuracy of eddy covariance evaporation measurements for three semiarid ecosystems. *Agricultural and Forest Meteorology* **150**: 219–225.

Scott RL, Watts C, Garatuza J, Edwards E, Goodrich D, Williams DG, *et al*. 2003. The understory and overstory partitioning of energy and water fluxes in an open canopy, semiarid woodland. *Journal of Agriculture and Forest Meteorology* **114**: 127–139.

Scott RL, Edwards EA, Shuttleworth WJ, Huxman TE, Watts C, Goodrich DC. 2004. Interannual and seasonal variation in fluxes of water and carbon dioxide from a riparian woodland ecosystem. *Agricultural and Forest Meteorology* **122**: 65–84.

Scott RL, Goodrich D, Levick L. 2006. Determining the riparian groundwater use within the San Pedro Riparian National Conservation Area and the Sierra Vista Subwatershed, Arizona. In *Hydrologic Requirements of and Consumptive Ground-Water Use by Riparian Vegetation along the San Pedro River, Arizona*, Leenhouts JM, Scott RL (eds). USGS Scientific Investigations Report 2005: 5163, United States Geological Survey, U.S. Department of Interior, Washington, D.C.; 107–152.

Scott RL, Cable WL, Huxman TE, Nagler PL, Hernandez M, Goodrich DC. 2008. Multiyear riparian evapotranspiration and groundwater use for a semiarid watershed. *Journal of Arid Environments* **72**: 1232–1246.

Serrat-Capdevil A, Scott RL, Shuttleworth WJ, Valdés JB. 2011. Estimating evapotranspiration under warmer climates: insights from a semiarid riparian system. *Journal of Hydrology* **399**: 1–11.

Serrat-Capdevila A, Valdes JB, Gonzalez-Perez J, Baird K, Mata LJ, Maddock T. 2007. Modeling climate change impacts—and uncertainty—on the hydrology of a riparian system: the San Pedro Basin (Arizona/Sonora). *Journal of Hydrology* **347**: 48–65.

Snyder KA, Williams DG. 2000. Water sources used by riparian trees varies among stream types on the San Pedro River, Arizona. *Agricultural and Forest Meteorology* **105**: 227–240.

Sorooshian S, Bales R, Gupta H, Woodard G, Washburne J. 2002. A brief history and mission of SAHRA: a National Science Foundation Science and Technology Center on "Sustainability of semi-arid hydrology and riparian areas". *Hydrological Processes* **16**: 3293–3295.

Stromberg JC, Tellman B (eds). 2009. *Ecology and Conservation of the San Pedro River*. University of Arizona Press: Tucson, AZ; 529.

Stromberg JC, Tiller R, Richter B. 1996. Effects of groundwater decline on riparian vegetation of semiarid regions: the San Pedro River, Arizona. *Ecological Applications* **6**: 113–131.

Stromberg JC, Lite SJ, Rychener TJ, Levick LR, Dixon MD, Watts JM. 2006. Status of the riparian vegetation in the Upper San Pedro River, Arizona: application of an assessment model. *Environmental Monitoring and Assessment* **115**: 145–173.

Stromberg JC, Dixon MD, Scott RL, Maddock T, Baird KJ, Tellman B. 2009a. Status of the Upper San Pedro River (USA) riparian ecosystem. In *Ecology and Conservation of the San Pedro River*, Stromberg JC, Tellman B (eds). University of Arizona Press: Tucson, AZ; 13–36.

Stromberg JC, Lite SJ, Dixon MD, Tiller RL. 2009b. Riparian vegetation: pattern and processes. In *Ecology and Conservation of the San Pedro River*, Stromberg JC, Tellman B (eds). University of Arizona Press: Tucson, AZ; 371–387.

Stromberg JC, Tluczek MG, Hazelton AF, Ajami H. 2010. A century of riparian forest expansion following extreme disturbance: spatio-temporal change in *Populus*/*Salix*/*Tamarix* forests along the Upper Sand Pedro River, Arizona, U.S.A. *Forest Ecology and Management* **259**: 1181–1189.

Tan B, Woodcock CE, Hu J, Zhang P, Ozdogan M, Huang D, *et al*. 2006. The impact of gridding artifacts on the local spatial properties of MODIS data: implications for validation, compositing, and band-to-band registration across resolutions. *Remote Sensing of Environment* **105**: 98–114.

Thomas BE, Pool DR. 2006. Trends in Streamflow of the San Pedro River, southeastern Arizona, and trends in precipitation and streamflow in northwestern New Mexico and southeastern Arizona. U.S. Geological Survey Professional Paper 1712, Reston, VI, 79 pp.

Webb RH, Leake SA, Turner RM. 2007. *The Ribbon of Green: Change in Riparian Vegetation in the Southwestern United States*. University of Arizona Press: Tucson, AZ.

Williams DG, Scott RL. 2009. Vegetation–hydrology interactions: dynamics of riparian plant water use. In *Ecology and Conservation of the San Pedro River*, Stromberg JC, Tellman B (eds). University of Arizona Press: Tucson, AZ; 37–56.

SUPPORTING INFORMATION

Additional supporting information may be found in the online version of this article at the publisher's web site.